

14 Surface Physics

M. Hengsberger, G. Mette, L. Castiglioni, H. Cun, S. Förster, E. Miniussi, C. Monney, R. Westerstöm, C. Bernard, M. Greif, A. Hemmi, P. Kliuiev, A. Kostanyan, G. Landolt, A. Schuler, R. Stania, WD. Zabka, R. Arulanantham, M. Baumgartner, D. Becker-Koch, M. Graf, A. Spescha, T. Kälin, T. Greber, and J. Osterwalder

The group investigates surface and interface phenomena at the atomic level. For this purpose the laboratory is well equipped for the preparation and characterization of clean single-crystalline surfaces as well as metal and molecular monolayer films, using a wide variety of experimental techniques. Moreover, the group is participating actively in the buildup and commissioning of the new SLS beam-line PEARL (PhotoEmission and Atomic Resolution Laboratory).

We hosted four postdocs with their own grants: H. Cun (UZH Forschungskredit): *Freestanding monolayers of boron nitride, graphene and their heterostructures*, S. Förster (P.R.I.M.E program of the DAAD): *Looking inside a 2D quasicrystal*, C. Monney (SNF Ambizione): *Time- and angle-resolved photoemission spectroscopy on correlated materials*, and R. Westerström (Swedish Research Council): *A new family of single-molecule magnets: Structural and magnetic characterization of self-assembled monolayers*.

During the report period the research was performed in the following four groups of projects:

- 2D Materials

The long term project on two dimensional (2D) materials progressed along two lines. First, high quality mono-atomic layers of hexagonal boron nitride were grown on single crystalline Rh(111) four-inch wafers [1] and distributed to eight users within and outside the Future and Emerging Technology (FET) Graphene flagship of the European Union. The group continued the efforts for the delamination of single orientation layers of graphene and hexagonal boron nitride from such transition metal substrates by electrochemical means. Second, we explore atom implantation beneath single layer materials by means of low energy ions. It turns out that the created defects, the "nanotents", harbor single atoms beneath an atomically thin "rainfly" and occupy preferential sites within the large 3 nm super unit cells of h-BN/Rh(111) [2, 3] and graphene on Ru(0001) [4]. The ion irradiation also enables the formation of 2 nm voids in single-layer h-BN and graphene, where we succeeded to construct a model for the remarkable nanostructure formation process via the "can-opener" effect, showing that the voids may be annihilated at higher temperatures [5].

- Ultrafast processes at surfaces

The Swiss National Science Foundation (SNF) granted the NCCR MUST (Molecular Ultrafast Science and Technology) for a second period of four years, starting in July 2014. We concluded our series of attosecond measurements in collaboration with ETH Zurich by taking RABBITT traces from various surfaces. Moreover, first time-resolved photoelectron diffraction data were taken from Bi(111). From these data it was possible to extract both electronic and structural dynamics underlying the excitation of coherent phonons in Bi. All these results are currently analyzed and will be submitted for publication in 2015 (see Sec. 14.1). Simulations on the time evolution of the orientation of CO molecules on Pt(111) were performed [6] (see Sec. 14.2). Within the Ambizione project of C. Monney we started to build up a new spectrometer for time-resolved measurements which will be located in the laser-laboratory. This spectrometer will be dedicated to time-resolved two-photon-photoemission experiments and, later on, time-resolved photoelectron spectroscopy experiments using a new high-harmonic gas jet source for obtaining high-energy UV-light [8].

- LightChEC

Within the University Research Priority Program "Light to Chemical Energy Conversion" (LightChEC), we are developing model systems for water reduction and oxidation catalysts, as well as photosensitizers supported on well-defined single-crystal surfaces, with the goal to identify suitable substrates and covalent anchoring units for a heterogeneous water splitting device. Metal complexes like cobalt-pyrphyrin have shown promise for water reduction in homogeneous catalysis [7]. The adsorption of the macrocyclic ligand pyrphyrin synthesized in the group of R. Alberto at UZH was studied on a Au(111) surface. The phase diagram of pyrphyrin on Au(111) in the sub-monolayer regime was established. Two distinct phases were identified and structurally characterized. On the high-coverage phase, deposition of Co atoms at the level of 5% of a monolayer and subsequent annealing lead to the formation of an almost complete monolayer of Co-ligated pyrphyrin molecules.

- Spin Shuttles

The investigation of endohedral single molecule magnets (spin shuttles) [9] was continued within the DACH project "Nitride Cluster Fullerene Spin Shuttles: The role of cluster composition for single molecule magnet behavior" in collaboration with IFW Dresden (A. Popov) and PSI Villigen (C. Piamonteze). With angular dependent x-ray absorption spectroscopy we could demonstrate that in a monolayer of Dy₂ScN@C₈₀ on Rh(111) the endohedral units (Dy₂ScN) orient parallel to the surface and show single molecule magnet behavior at 4 K [10] (see Sec. 14.3). We also installed and commissioned the sub-Kelvin SQUID magnetometer at Irchel (ASKUZI), a joint project with the group of A. Schilling and G. Patzke. Several new endohedral single molecule magnets were found and are further investigated.

[1] A. Hemmi *et al.*, Rev. Sci. Instr. **85**, 035101 (2014).

[2] H. Cun *et al.*, ACS Nano **8**, 1014 (2014).

[3] H. Cun *et al.*, Nano Lett. **13**, 2098 (2013).

[4] H. Cun *et al.*, Surf. Sci. **634**, 95 (2015).

[5] H. Cun *et al.*, ACS Nano, **8**, 7423 (2014).

[6] M. Greif, Ph.D. Thesis, University of Zurich (2015).

[7] S. Schnidrig *et al.* in preparation.

[8] C.M. Heyl, *et al.*,
J. Phys. B: At. Mol. Opt. Phys. **45**, 074020 (2012).

[9] R. Westerström *et al.*,
J. Am. Chem. Soc. **134**, 9840 (2012).

[10] R. Westerström *et al.*,
Phys. Rev. Lett. **144**, 087201 (2015).

60

In the following, three highlights of last year's research are presented in more detail.

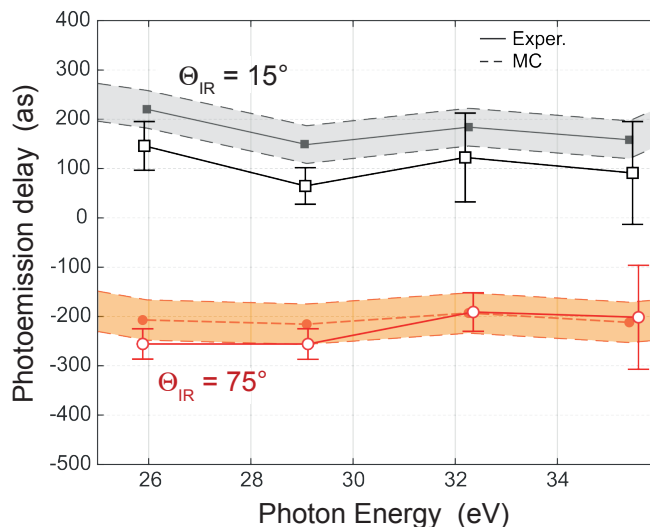
FIG. 14.1 – Delays extracted from the RABBITT traces at two equivalent points in the Brillouin zone of Cu(111), which correspond to angles of light incidence $\Theta_{IR} = 15^\circ$ and 75° (see text). The results of semi-classical Monte Carlo calculations are shown for comparison where the shaded regions represent the uncertainty in the gas phase reference measurement used for time delay calibration. The absolute delay offset is not known, but only the shift between the two incidence angles is important. For this reason the theoretical results were shifted to fit the measurements. From Ref. [5].

14.1 Photoemission delays from attosecond interferometry

In collaboration with: Matteo Lucchini, Lamia Kasmi, Lukas Gallmann, and Ursula Keller (Attoline project), Physics Department, ETH Zurich; NCCR MUST.

We continued to take RABBITT measurements from noble metal surfaces in collaboration with the group of U. Keller at Attoline (ETHZ). RABBITT, which stands for reconstruction of attosecond beating by interference of two-photon transitions [1] was initially used in gas-phase experiments to study atomic photoemission delay at the attosecond time scale [2]. In RABBITT, the absorption of an XUV photon with a specific energy is followed by either absorption or stimulated emission of an IR photon. This two-photon process gives rise to the appearance of sidebands in the temporal overlap of the XUV and IR pulses. Quantum path interference leads to a beating pattern that entails the spectral photoemission phase. The extension of RABBITT to noble-metal surfaces allowed us to extract energy-dependent photoemission delays from interferometric pump-probe experiments using a short attosecond pulse train in the XUV as pump pulse and a few cycle IR probe pulse [3]. The main advantages compared to so-called streaking experiments [4] are the use of fairly long IR pulses and attosecond pulse trains. This simultaneously maximizes the energy *and* temporal resolution without being limited by the time-bandwidth product.

From our previous study [3] one important problem remained to be solved: The description of the transient optical grating generated by incoming and reflected IR fields. We addressed the open question of the effect of the IR probing field and the phase of the transient grating by taking traces from Cu(111) [5]. In order to do so, it was necessary to exclude additional contributions from the photoemission process itself. Therefore, the traces were obtained from equivalent momenta in the Cu Brillouin



zone on the two sides of a mirror plane of the Cu(111) surface. The electrons originate from the same initial states and are excited in identical final states for the two geometries. The only difference is the angle of light incidence and, thereby, a difference in transient grating. The phase will change as well as a consequence of the complex angle-dependent reflection coefficient. As a result, the phase shift observed for the two geometries equals almost exactly the phase difference computed using Fresnel's equations and that of published values for the reflection coefficient at 800 nm, as shown in Fig. 14.1.

- [1] P. M. Paul *et al.*, *Science* **292**, 1689 (2001).
- [2] K. Klünder *et al.*, *Phys. Rev. Lett.* **106**, 143002 (2011).
- [3] R. Locher, L. Castiglioni *et al.*, *Optica* **2**, 405 (2015).
- [4] A. Cavalieri *et al.*, *Nature* **449**, 1029 (2007).
- [5] M. Lucchini *et al.*, submitted for publication (2015).

14.2 Recording molecular motion by photoelectron diffraction

In collaboration with: Tibor Nagy, Maxym Soloviov, and Markus Meuwly, University of Basel; NCCR MUST.

Time-resolved photoelectron diffraction experiments became possible with the availability of ultrashort extreme ultraviolet pulses or x-ray pulses from free-electron lasers [1, 2]. In view of future time-resolved investigations of THz-driven molecular dynamics the group of M. Meuwly (U Basel) and our group simulated the behavior of 50 independent carbon monoxide molecules adsorbed on on-top positions on a Pt(111) surface [3]. Platinum is a well established and efficient catalyst for reactions of CO [4]. There have been many studies of the system CO on Pt(111) with different experimental methods [5]. For low coverage, the molecules adsorb exclusively on energetically favored on top-sites of the platinum surface. With increasing coverage the work function of the CO/Pt(111) system first reaches a minimum at a coverage of $\Theta = 1/6$,

followed by a continuous rise for larger coverage. This behavior was explained by different dipole moments of CO at the two different adsorption sites [6].

For a 1/6 coverage the dipole moments of the molecules point along the CO axis [7, 8]. In this configuration THz-radiation is believed to excite a coherent wagging motion of CO molecules at about 1.8 THz [9]. The 50 simulated molecular trajectories represent atomic coordinates over a temporal range of about 25 ps in steps of 10 fs which were used as input in our single-scattering cluster code. The output of 50 files per time step, summed up incoherently, constitute the simulated experimental photoelectron diffraction pattern. For the simulations, emission out of the C 1s level was assumed using 1 keV x-ray pulses. The electrons undergo scattering at the oxygen atom located above. As a result, the angular distribution of the photoemission intensity exhibits a maximum for the angle of the C-O-bond for each single trajectory. However, since photoelectron diffraction integrates over a large spot and therefore over many molecules, the thermal motions of the molecules are averaging out for negative delays. The THz field aligns and amplifies the motion and induces a coherent combined hindered translation and rotation, well observable by photoelectron diffraction from the C 1s level [3], as shown in Fig. 14.2.

61

- [1] M. Greif *et al.*, *J. El. Spec. Rel. Phen.* **197**, 30 (2014).
- [2] M. Greif, Ph.D. Thesis, University of Zurich (2015).
- [3] M. Greif, T. Nagy *et al.*, submitted to *Struct. Dyn.* (2015).
- [4] I. Langmuir, *Trans. Faraday Soc.* **17**, 621 (1922).
- [5] Y. Y. Yeo, L. Vattuone, and D. A. King, *J. Chem. Phys.* **106**, 392 (1997).
- [6] G. Ertl, M. Neumann, and K. Streit, *Surf. Sci.* **64**, 393 (1977).
- [7] H. Ueba, *Surf. Sci.* **188**, 421 (1987).
- [8] P. Deshlahra, J. Conway, E. E. Wolf, and W. F. Schneider, *Langmuir* **28**, 8408 (2012).
- [9] B. Patterson *et al.*, *Europhys. News* **41**, 28 (2010).

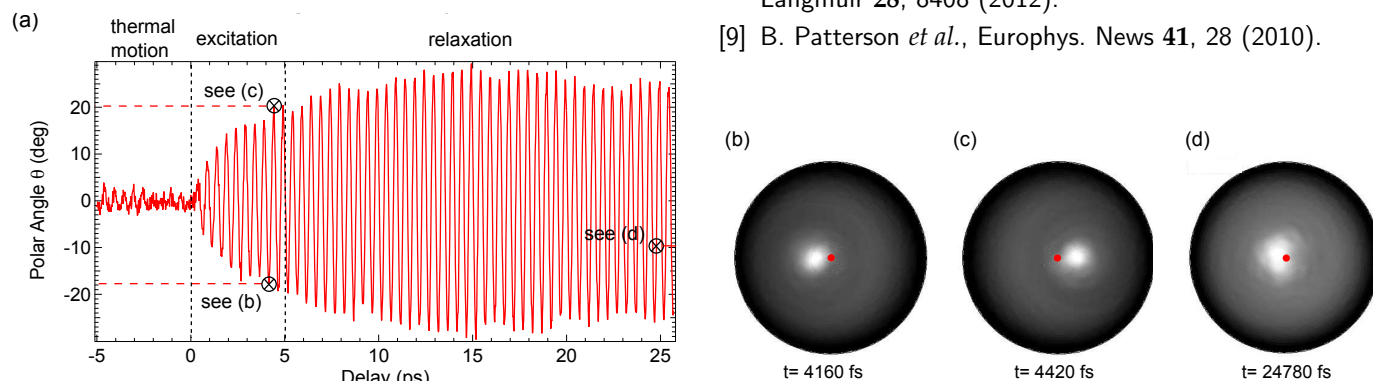


FIG. 14.2 – Results of molecular force field and electron single-scattering calculations, averaged over 50 independent molecular trajectories [3]. (a): angular position of the intensity maximum representing the orientation of the C-O-bond with respect to the surface normal. (b) - (d): diffraction patterns at the indicated delays after the THz excitation pulse. (b) and (c) highlight the orientation of the molecules at different extrema of the coherent oscillation.

14.3 Magnetic hysteresis and anisotropy of metallofullerene nanomagnets on a surface

in collaboration with: Alexey Popov, IFW Dresden; Cinthia Piamonteze, Jan Dreiser, and Bernard Delley Paul Scherrer Institut, Villigen.

The hollow interior of the fullerene [1] carbon cage can be used to encapsulate paramagnetic systems consisting of single atoms [2]. A fascinating example is the dysprosium-scandium based endofullerene-series $\text{Dy}_n\text{Sc}_{3-n}\text{N}@C_{80}$ ($n = 1, 2, 3$) where the different stoichiometries result in distinct ground-state properties like tunneling of magnetization ($n = 1$), remanence ($n = 2$), or frustration ($n = 3$) [3, 4]. Interaction with the ligand fields, mainly from the central N^{3-} ion, imposes an axial anisotropy that restricts the Dy moments to orient along the magnetic easy-axis directed parallel to the corresponding Dy-N bonds. Moreover, the ligand field splits the $2J+1$ degenerate ground state into states separated by an energy barrier that prevents a spontaneous reversal of the magnetization. In the case of the di-dysprosium compound (Fig. 14.3), exchange and dipolar coupling between the two magnetic moments stabilizes hysteresis and a large remanence with a relaxation time of one hour at 2 K are found [4]. These endofullerenes belong to the group of single-molecule magnets [5, 6], a class of molecules that exhibits an intrinsic magnetic bistability at low temperatures. They are particularly promising for molecular spintronics applications [7] and quantum computing [8]. Applications will require that the molecules are transferred from the bulk phase and deposited onto substrates or integrated into different device architectures. Therefore, it is of interest to know how the molecular magnetic properties are modified at low coverages on surfaces.

In order to investigate how the proximity of a metal surface influences the ordering of the magnetic cluster and the magnetic bistability, we have studied molecular films of $\text{Dy}_2\text{ScN}@C_{80}$ on a rodium metal surface [9].

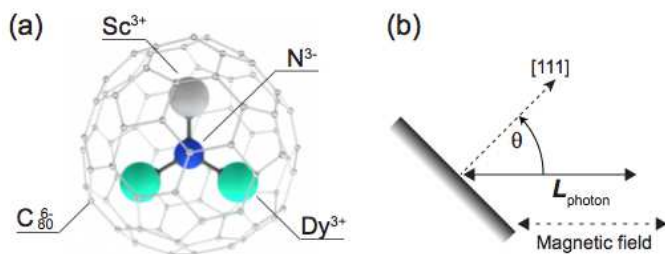


FIG. 14.3 –

(a) Ball-and-stick model of $\text{Dy}_2\text{ScN}@C_{80}$.

(b) Measurement geometry with the angular momentum of the x-rays L_{ph} , parallel or antiparallel to the magnetic field and at an angle of θ with respect to the normal of the sample surface.

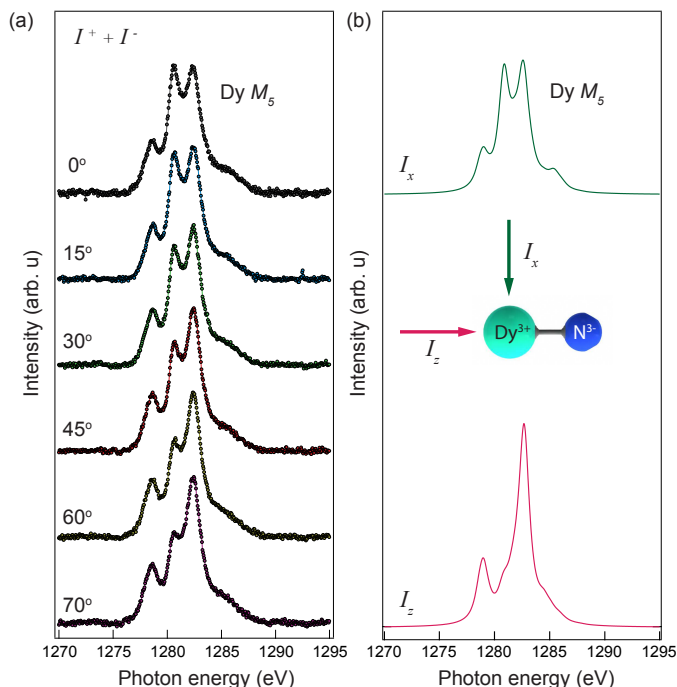


FIG. 14.4 –

(a) XAS measured at the Dy M_5 -edge from a sub-ML of $\text{Dy}_2\text{ScN}@C_{80}/\text{Rh}(111)$ $T = 4$ K, $\mu_0 H = 6.5$ T, measurement geometry in Fig. 14.3 (b). Each data set is normalized to the integrated intensity.

(b) Calculated absorption with the x-ray beam and external field oriented parallel I_z , and perpendicular I_x , to the magnetic easy-axis (Dy-N bond).

For a sub-monolayer coverage is a significant change in the Dy XAS spectra observed as the angle between the surface normal and the x-ray beam is varied (Fig. 14.4 (a)). This effect is a consequence of an anisotropic charge distribution of the 4f orbitals due to a preferential orientation of the Dy_2ScN cluster. A comparison with multiplet calculations reveals that the cluster adopts an orientation parallel to the surface (Fig. 14.4 (b)). Combined with the local magnetic easy axis for the encapsulated Dy ions, the structural orientation of the cluster in the sub-monolayer results in surface aligned magnetic moments and a macroscopic anisotropy [9].

The magnetism of the system was studied by x-ray magnetic circular dichroism (XMCD), a spectroscopy technique that probes the magnetic moments of the individual Dy ions [3]. By measuring the XMCD signal while sweeping the magnetic field, element specific magnetization curves can be recorded. Figure 14.5 displays magnetization curves recorded from a sub-monolayer and a multilayer at 4 K. Hysteresis is observed for both systems, demonstrating that the corresponding magnetic relax-

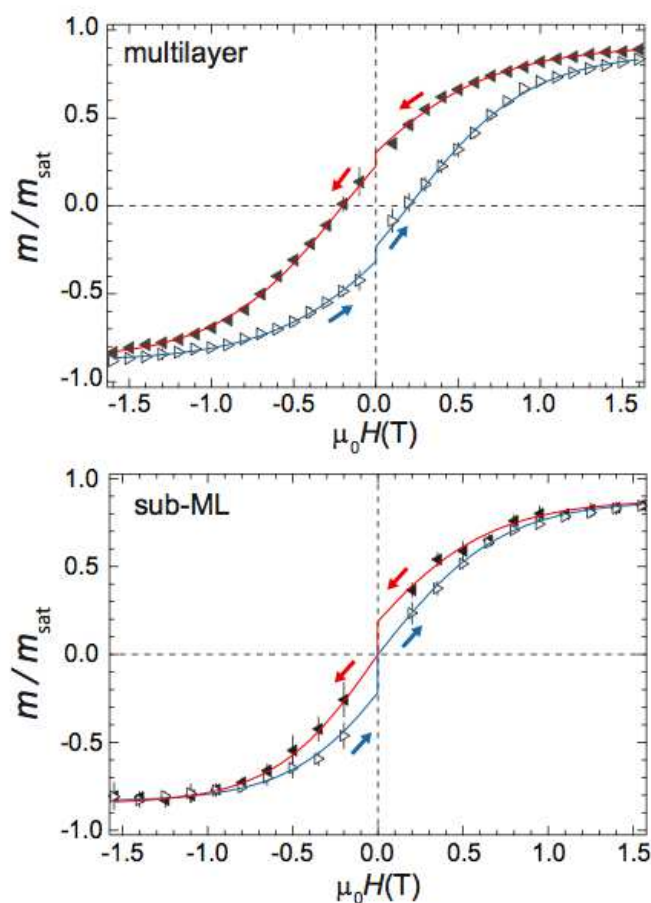


FIG. 14.5 – Hysteresis curves measured from a multilayer and a sub-ML of $\text{Dy}_2\text{ScN}@C_{80}/\text{Rh}(111)$ at a magnetic field sweep rate of 2 T/min and a sample temperature of ~ 4 K. The data were recorded with the x-ray beam and the magnetic field at an incidence angle of $\theta = 60^\circ$. The magnetization curves correspond to the average of several independent measurements, where the error bars are the standard deviations at each external magnetic field setting. The arrows indicate the ramping direction of the magnetic field, the lines are guides to the eye, and m_{sat} is the saturated magnetisation at ≈ 6.5 T. The drop in magnetization at zero field results from the ≈ 30 s it takes to switch the polarity of the magnet.

ation times are slow compared to the measurement time. However, comparing the magnetization curves from the two systems indicates that the magnetic bi-stability of $\text{Dy}_2\text{ScN}@C_{80}$ is modified by the proximity of the rhodium metal surface. The comparison to the thicker film (representative of the bulk phase), allows to estimate that the proximity of the metal surface results in four times higher relaxation rates and in a resulting remanence time of about 30 s [9].

In summary, angle dependent XAS from a sub-ML of $\text{Dy}_2\text{ScN}@C_{80}$ on $\text{Rh}(111)$ reveal a one-to-one correspondence between structural and magnetic ordering: The combined effect of the local magnetic easy-axis for the encapsulated Dy ions, and the preferred absorption geometry of the endohedral cluster, indicates a bistable surface aligned macrospin.

- [1] H. Kroto *et al.*, *Nature*, **318**, 162 (1985).
- [2] A. Popov *et al.*, *Chem. Rev.* **113**, 5989 (2013).
- [3] R. Westerström *et al.*, *J. Am. Chem. Soc.* **134**, 9840 (2012).
- [4] R. Westerström *et al.*, *Phys. Rev. B.* **89**, 060406(R) (2014).
- [5] R. Sessoli, *et al.*, *Nature* **365**, 141 (1993).
- [6] D. Gatteschi *et al.*, *Molecular Nanomagnets*, Oxford University Press, New York, (2006).
- [7] L. Bogani *et al.*, *Nat Mater* **7**, 179 (2008).
- [8] M. N. Leuenberger *et al.*, *Nature* **410**, 789 (2001).
- [9] R. Westerström *et al.*, *Phys. Rev. Lett* **144**, 087201 (2015).